

# Investigation of Reddening in Fields of the SMASH Survey

Elizabeth A. Juelfs<sup>1</sup> & Knut Olsen<sup>2</sup>

<sup>1</sup>Austin Peay State University, Clarksville, TN, <sup>2</sup>National Optical Astronomy Observatory, Tucson, AZ

ejuelfs@my.apsu.edu



## Abstract

We present dust extinction maps derived from eight fields in the Survey of the Magellanic Stellar History (SMASH), a survey that is imaging  $480\text{deg}^2$  of the southern sky in DES-ugriz with the CTIO 4-m Blanco telescope and the Dark Energy Camera (DECam). We derive the extinction due to dust using fits to the stellar locus of stars brighter than  $g=21$  in color-color diagrams, and explore the spatial distribution of the extinction within each of the fields. We compare our results to the extinction map of Schlegel, Finkbeiner, & Davis (1998), and find generally good agreement. We describe plans to measure the three-dimensional distribution of extinction in these fields using fainter stars and background galaxies as tracers.

## Introduction

SMASH is a survey of the Magellanic periphery containing 180 fields intended to map stellar debris and extended populations, and will search for stellar components of the Magellanic Stream and the Leading Arm. SMASH will be important for understanding the history and consequences of Magellanic interactions as explained in the Nidever, et al. (2013) proposal. The Magellanic Clouds are the nearest interacting galaxy system to the Milky Way and are believed to be on their first infall into the Milky Way. Figure 1 shows the fields of SMASH.

The effect of dust on the photometry must first be evaluated to analyze the data from SMASH. Reddening occurs when light passes through dust or gas and is either absorbed or scattered, making objects appear dimmer than their absolute magnitudes. Dust absorbs and scatters light at all wavelengths; however, more extinction occurs at higher energy wavelengths.

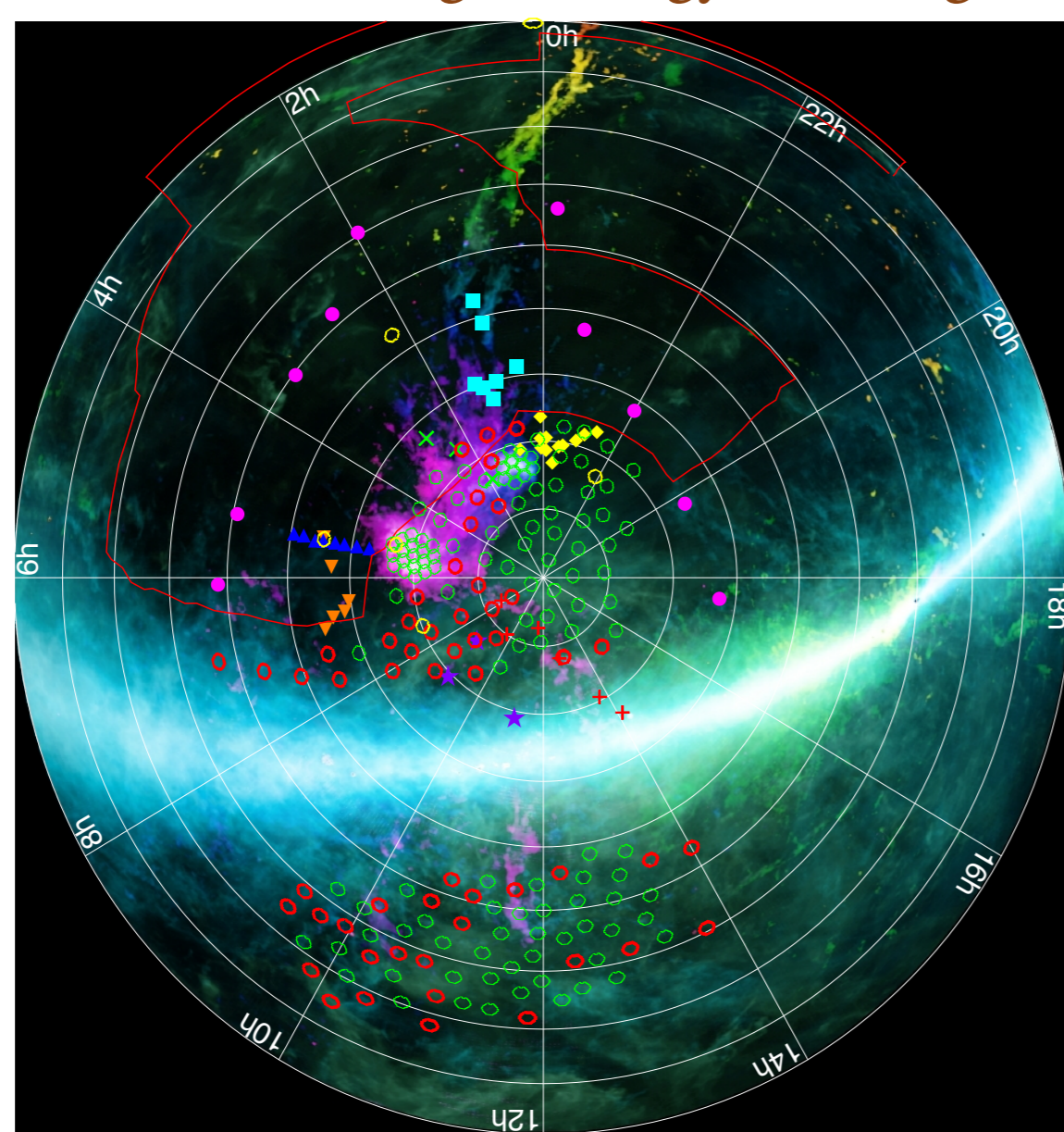


**Figure 1:** SMASH survey fields. The green circles are the fields that had been observed as of December 2014, and the red circles are those fields that still needed to be observed.

## Methods: Color-Color Diagrams as a Diagnostic for Reddening

Color-color and color-magnitude diagrams were constructed for each of the 62 chips in each of the eight fields examined for this project. In a color-magnitude diagram for a field from SMASH (seen on the left image of Figure 2), several distinct features can be seen such as: close proximity stars in the Milky Way, faint background galaxies in the high density area on the lower portion of the diagram, and the blue end of the main sequence near the top of the color-magnitude diagram.

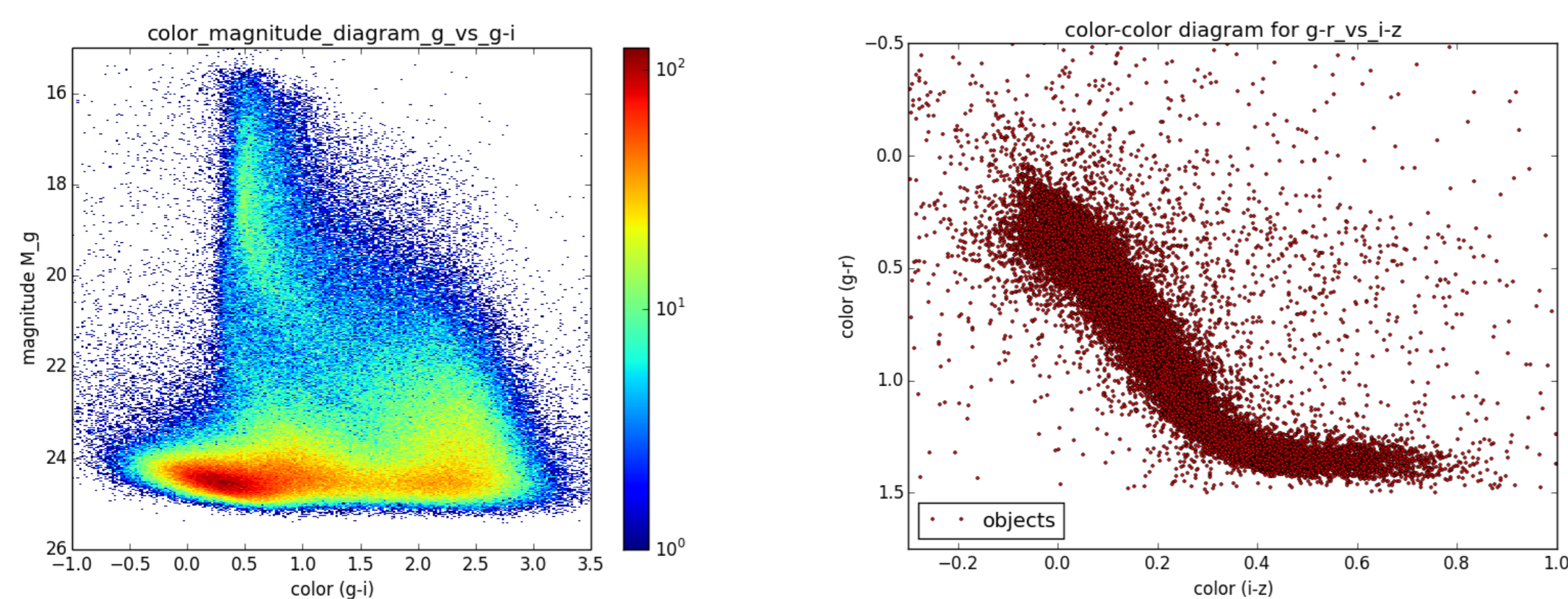


**Figure 2:** Color-Magnitude Diagram for all magnitudes (Magnitude in  $g$  versus color index  $g-i$ ) and Color-Color Diagram for objects brighter than 21 magnitude in  $g$  (Color index  $g-i$  versus color index  $i-z$ ) for field 7 of SMASH.

A color-magnitude diagram looks through the disk of the galaxy, and objects are seen to be distributed over a wide range of distances, making objects appear in different places than if all objects were at absolute magnitude. In order to avoid the effect of varied distances, color-color diagrams were used to investigate the effects of reddening. Color-color diagrams show a population of objects at apparent magnitudes as a function of various wavelengths. The right-hand image of Figure 2 shows the color-color diagram from field 7.

The color-color diagrams for each field were constrained to look at the brighter objects, and were fitted with a curve using a running median method so that differences among the plots of each chip would be easily determined. The left image of Figure 3 shows the color-color diagram for field 7 with the median fit curve and the reddening vector over-plotted. It is interesting to note that the blue end of the color-color sequence runs almost parallel to the reddening vector. The red end does not, so it can be used to look at reddening.

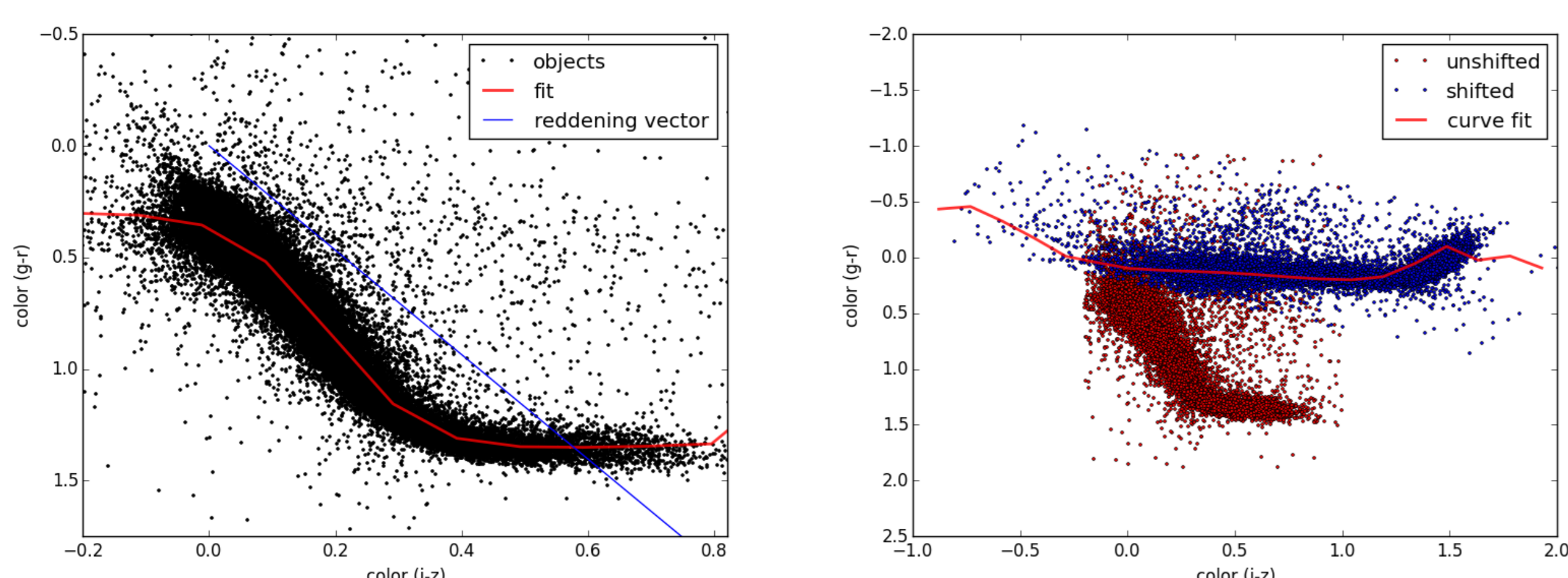


**Figure 3:** Color-Color Diagram for field 7 of SMASH for objects brighter than 21 magnitude in  $g$  over-plotted with the median fit curve (in red) and the reddening vector (in blue), and Color-Color Diagram for field 7 of SMASH for objects brighter than 21 magnitude in  $g$  and shifted Color-Color Diagram for same population with over-plotted median fit curve

Once the color-color diagrams of each field were fit with a curve, they were shifted so that one axis aligned with the horizontal axis of the plot. This rotation process (seen in the right-hand image of Figure 3) was done using a rotation matrix with an angle found by taking the tangent of the slope of the reddening vector (valued at 2.34), which corresponds to the standard reddening law.

Next, each field was evaluated by comparing the field-wide fit curve to the fit curve for each chip. Finding the difference between the horizontal positions of the bends of the curves for each chip as compared to the entire field represents the difference due to reddening.

Once the effect of dust had been determined for each chip, spatial distribution over each field was examined by viewing a right ascension and declination plot with the amount of horizontal separation between the knees of the fit curves (the effect of reddening) as a third axis for a surface plot (Figure 4).

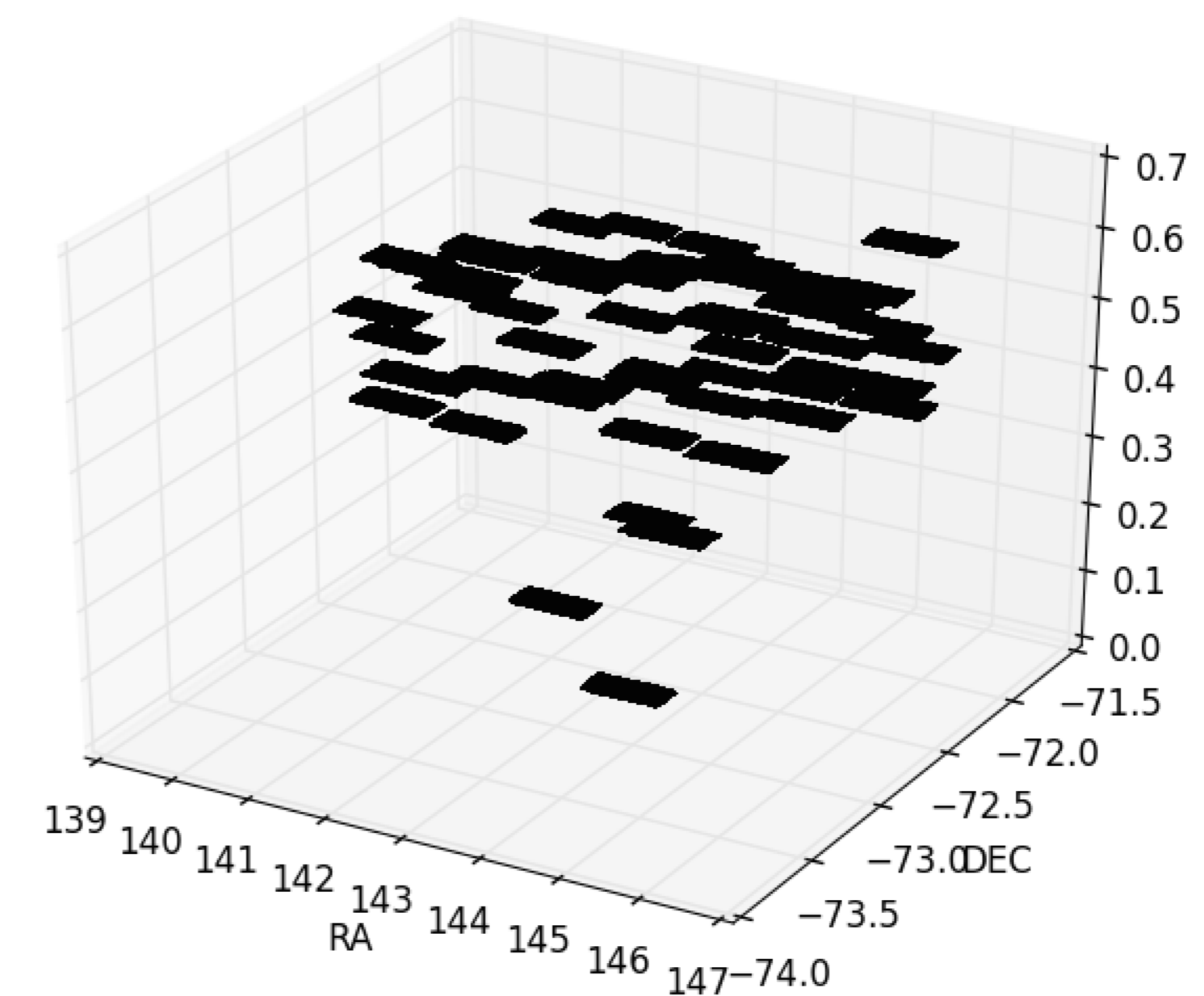


**Figure 4:** Spatial distribution of reddening for field 7

The computed reddening values were then compared with those of the map of Schlegel, Finkbeiner, & Davis (1998) by plotting the computed reddening values with the SFD  $E(B-V)$  values from the fits files for each field. The conversion between the calculated reddening values and  $E(B-V)$  was done using

$$\frac{(\Delta i-z)^2}{E(B-V)^2} + \frac{(\Delta g-r)^2}{E(B-V)^2} = \frac{x^2}{E(B-V)^2}$$

where  $x$  is the calculated reddening value. These  $E(B-V)$  values were plotted versus the  $E(B-V)$  values from the SFD map. A line of best fit was then over-plotted to look at the correlation between the two sets of  $E(B-V)$  values.

## Results and Conclusions

This process was used on 8 of the 180 fields. Figure 5 shows the correlation between the reddening values calculated and the corresponding values from the SFD map.

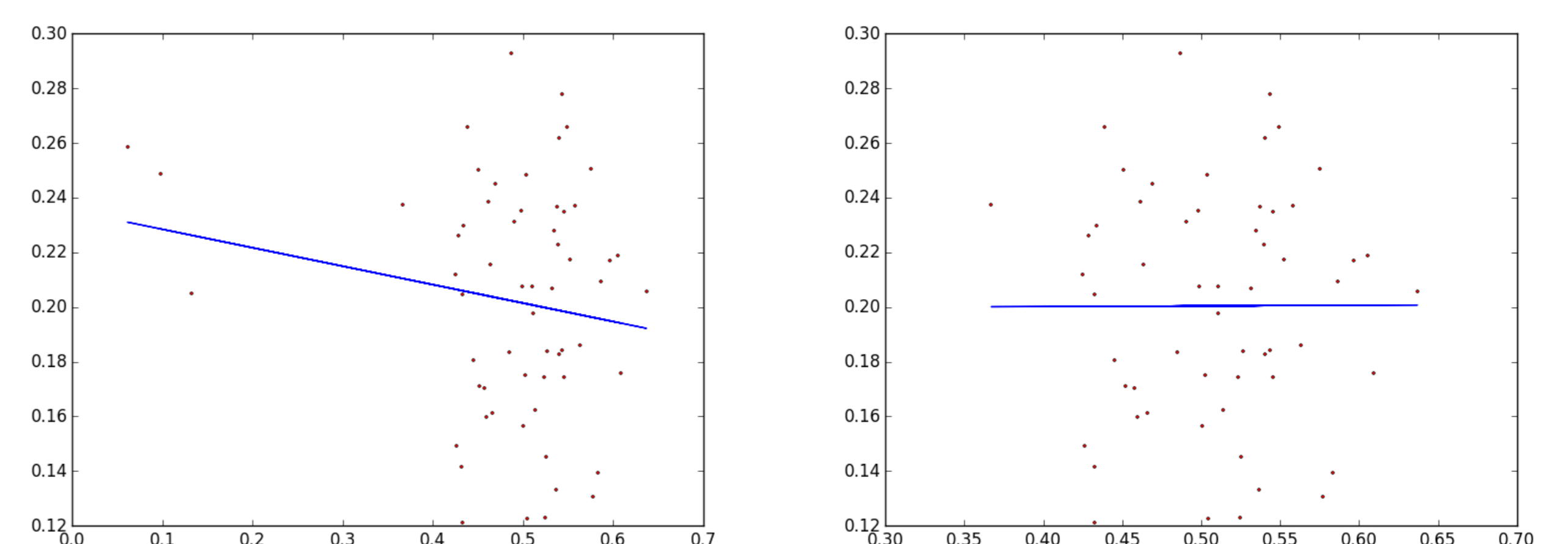


**Figure 5:** Scatter plot of SFD  $E(B-V)$  versus calculated  $E(B-V)$  values for field 7, and Scatter plot of SFD  $E(B-V)$  versus calculated  $E(B-V)$  values for field 7 with outliers removed

The left image of Figure 5 shows the scatter plot of the SFD  $E(B-V)$  versus calculated  $E(B-V)$  values over-plotted with a line of best fit.

After removing outliers from the scatter plot of the SFD  $E(B-V)$  versus calculated  $E(B-V)$  values, the correlation between the two sets of values was improved in 6 of the 8 fields tested. The right-hand image of Figure 5 shows the scatter plot of the SFD  $E(B-V)$  versus calculated  $E(B-V)$  values with the outliers removed.

## Forthcoming Research

This project will be continued using different color combinations for color-color diagrams. The perpendicular differences between the field wide and chip-specific fit curves need to be analyzed. The depth of the reddening analysis can also be expanded by extending the fainter end of the range of magnitudes used for analysis to 24th magnitude from 21st magnitude. The relationship between extinction and magnitude will also be explored. Extinction will also be found for each star rather than just the average reddening for each chip.

## References

- [1] Nidever, D., et al. 2013, NOAO Observing Proposal 2013B-0440
- [2] Schlegel, D. J., Finkbeiner, D. P., & Davis, M. 1998, ApJ, 500, 525

## Acknowledgements

Juelfs was supported by the NOAO/KPNO Research Experiences for Undergraduates (REU) Program which is funded by the National Science Foundation Research Experiences for Undergraduates Program (AST-1262829).